



Air-sea gas exchange in the central Baltic Sea

Ryo Dobashi¹, David T. Ho¹, Yuanxu Dong^{2,3}, Christa A. Marandino², Helen Czerski⁴

¹Department of Oceanography, University of Hawai'i at Mānoa, 1000 Pope Road, Honolulu, Hawaii 96822, USA

²GEOMAR Helmholtz Centre for Ocean Research Kiel, Research Division 2, Wischhofstr. 1-3, 24148, Kiel, Germany

5 ³Institute of Environmental Physics, Heidelberg University, Im Neuenheimer Feld 229, 69120 Heidelberg, Germany

⁴Department of Mechanical Engineering, University College London, Roberts Engineering Building, Torrington Place, London WC1E 7JE, United Kingdom

10 *Correspondence to:* Ryo Dobashi (rdobashi@hawaii.edu)

Abstract. Air-sea CO₂ fluxes play an important role in the global carbon cycle and impact Earth's climate. Knowledge of the gas transfer velocity (k) is needed to determine air-sea CO₂ fluxes, and wind speed-based parametrizations of k often perform well in the open ocean under moderate winds. In the Baltic Sea, several parameterizations have been proposed to estimate k , and they yield a higher k compared with parameterizations commonly used in the open ocean. In this study, we measured k in the Baltic Sea using the ³He/SF₆ dual tracer technique to assess the applicability of published parameterizations in the inland sea ecosystem. Observed k was similar to those in offshore regions at the same wind speeds, even with enhanced surfactant activity. Comparison with observations in the nearshore Baltic Sea suggests that commonly used open ocean parameterizations are applicable in the Baltic Sea under moderate wind speeds and developed wave fields.

1 Introduction

20 1.1 The role of air-sea gas exchange and k in the climate system

Air-sea gas exchange is a crucial part of the global biogeochemical processes, shaping the distribution and movement of gases across the Earth's two major reservoirs. The air-sea carbon dioxide (CO₂) exchange is particularly important because it influences the global climate. Atmospheric CO₂ contributes to global warming as a greenhouse gas, while oceanic CO₂ uptake serves as a major long-term sink. Between 2014 and 2023, 10.8 GtC yr⁻¹ of anthropogenic carbon was emitted to the atmosphere, while 2.9 GtC yr⁻¹ of the carbon was absorbed by the ocean, which stores 37,000 GtC of dissolved inorganic carbon (Friedlingstein et al., 2025). The determination of the air-sea CO₂ exchange needs the gas transfer velocity (k), which represents the kinetic control on the exchange and is a challenging parameter to measure directly in oceanic environments.

Extensive research has been conducted to understand the factors controlling air-sea gas exchange in order to parameterize k from readily measurable environmental parameters. Among these, wind speed has been the most effective variable for estimating k over the open ocean, where most gas exchange studies to date have been performed. Wind is so effective because it drives the two primary mechanisms governing air-sea gas exchange: near-surface turbulence and bubble formation



due to wave breaking (Wanninkhof et al., 2009). Additionally, wind speed is easily and frequently measured, and it is also readily available from remote sensing and included as a standard variable in models, making it highly practical for use in parameterizations. Under moderate wind speeds, commonly used wind speed/ k parameterizations such as those proposed by Nightingale et al. (2000a), Ho et al. (2006), and Wanninkhof (2014) can explain over 80% of the variance of $k(600)$ in the coastal and open oceans (Ho et al., 2011; Ho and Wanninkhof, 2016).

1.2 Measurement of k in the Baltic Sea

The Baltic Sea, situated in northern Europe, is an inland sea whose drainage basin is approximately four times larger than the sea itself, supporting a population of around 85 million people (Kuliński et al., 2022). Previous researchers have developed parameterizations to estimate k for the Baltic Sea based on waterside CO₂ mass balances (Kuss et al., 2004) and eddy covariance (EC) CO₂ from fixed towers in the Baltic (Weiss et al., 2007; Rutgersson and Smedman, 2010) (Table 1). The two (quadratic and cubic) parameterizations by Kuss et al. (2004), as well as that by Weiss et al. (2007), all yield significantly higher k than measurements using ³He/SF₆ in coastal and open oceans (Fig. 1). The parameterization by Rutgersson and Smedman (2010) is not included in Fig. 1 because they separated k into k_{wind} and $k_{\text{convection}}$, which are wind-driven k and water convection-driven k , respectively. Recently, Gutiérrez-Loza et al. (2022) investigated k measured from EC CO₂ over nine years at a fixed site on land in the central Baltic Sea. They found that, on average, the measured k followed the commonly used parameterization by Wanninkhof (2014). However, on shorter timescales, they also observed higher k compared with commonly used parameterizations for the coastal and open oceans.

Observational and modeling studies conducted over the last decade in the Baltic Sea to examine biogeochemical cycles, where fluxes of CO₂ and O₂ need to be quantified, have utilized a variety of wind speed/ k parameterizations (Table 2). However, k derived from different parameterizations can differ by more than a factor of 2. This difference in k means that the choice of an appropriate parameterization could significantly impact the conclusions of these biogeochemical studies. The objectives of this study are to determine gas transfer velocities in the central Baltic Sea, assess the applicability of published parameterizations in this region, and examine factors that drive air-sea gas exchange in this inland sea ecosystem.

2. Methods

2.1 CenBASE experiment

The Central Baltic Air-Sea Exchange Experiment (CenBASE) was conducted on board the R/V Elisabeth Mann Borgese (research cruise EMB295) from June to July 2022, in an area of the central Baltic Sea east of Gotland, Sweden (Fig. 2). During the cruise, k was measured using two methods: 1) ³He/SF₆ dual tracers; and 2) CO₂ eddy covariance. Underway SF₆ and acoustic doppler current profiler (ADCP) measurements were employed to investigate the spatial distribution and



Table 1. Gas transfer velocities determined from published parameterizations.

References	Parameterization for $k(600)$ or $k(660)$ (cm h ⁻¹)	Mean $k(600)$ (cm h ⁻¹)	cvRMSE
Nightingale et al. (2000)	$k(600)=0.333u_{10} + 0.222u_{10}^2$	12.0±4.0	6.2%
Ho et al. (2006)	$k(600)=0.266u_{10}^2$	11.7±4.4	6.6%
Wanninkhof et al. (2009)	$k(660)=3+0.1u_{10} + 0.064u_{10}^2 + 0.011u_{10}^3$ $k(660)=0.24u_{10}^2$	10.3±3.3	7.3%
Wanninkhof (2014)	$k(660)=0.251u_{10}^2$	11.6±4.3	6.6%
Reichl and Deike (2020)	$k(660)=0.775 \times 3.6 \times 10^5 \times (1.55 \times 10^{-4}u_* + k_{wb})$	11.9±2.7	5.3%
Yang et al. (2022)	$k(660)=0.36+1.203u_{10}+0.167u_{10}^2$	16.4±4.3	19.9%
Yang et al. (2024)	$k(660)=54.72u_*+10.44u_*H_s$	15.9±3.5	18.3%
Kuss et al. (2004) quadratic	$k(660)=0.45u_{10}^2$	20.8±7.7	29.8%



Kuss et al. (2004) cubic	$k(660)=0.037u_{10}^3$	11.8±7.0	10.1%
Weiss et al. (2007)	$k(660)=0.365u_{10}^2+0.46u_{10}$	20.0±6.8	28.6%
Rutgersson and Smedman (2010)	$k(660)=0.24u_{10}^2+k_c$	23.0±4.3	32.9%

The mean with standard deviation of the measured $k(600)$ were $10.8 \pm 2.9 \text{ cm h}^{-1}$.

k_{wb} in Reichl and Deike (2020) is $\frac{(1 \pm 0.2) \times 10^{-5}}{K_0 R T_0} u_*^{\frac{5}{3}} (g H_s)^{\frac{2}{3}}$, where K_0 is the solubility, R is the ideal gas constant, T_0 is the sea surface temperature, u_* is wind friction, g is gravitational acceleration, and H_s is the significant wave height.

k_c in Rutgersson and Smedman (2010) is $(B \cdot z_{ml})^{\frac{1}{3}}$, where B is the water side buoyancy flux calculated following Rutgersson and Smedman (2010) and z_{ml} is MLD.

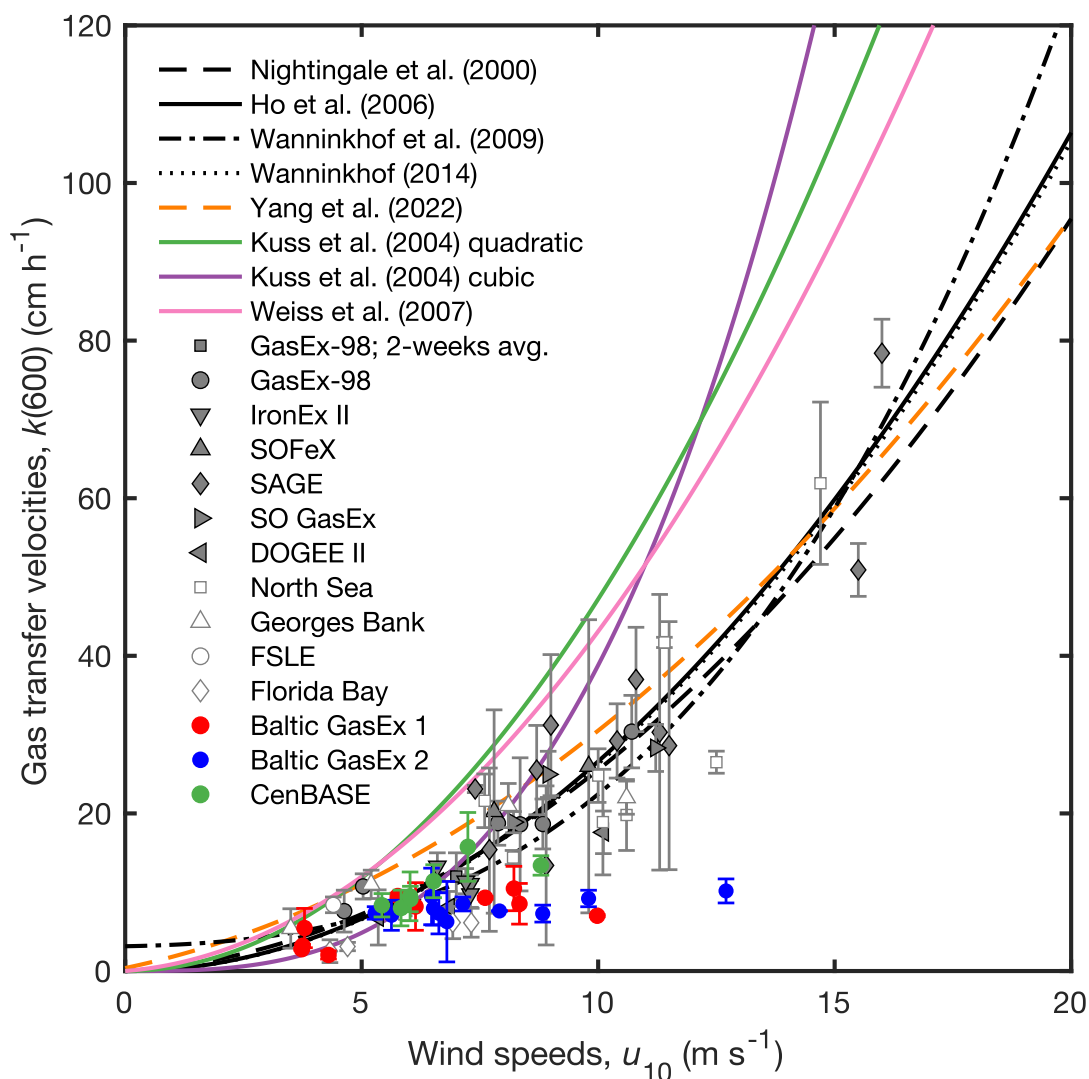


Figure 1: $k(600)$ (units: cm h^{-1}) derived from $^3\text{He}/\text{SF}_6$ dual-tracer experiments with wind speed at 10 m height (units: m s^{-1}). Results from CenBASE are green symbols. Red and blue symbols represent results from Baltic GasEx 1 and 2 from Dobashi et al. (2026). Solid gray symbols are for open ocean experiments; open symbols are for coastal and shelf experiments. The North Sea data are from Nightingale et al. (2000a), Georges Bank data are from Wanninkhof et al. (1993) and reanalyzed by Asher and Wanninkhof (1998), Florida Shelf Lagrangian Experiment (FSLE) data are from Wanninkhof et al. (1997), Florida Bay data is from Dobashi and Ho (2023), GasEx-98 are from McGillis et al. (2001), IronEx II data are from Nightingale et al. (2000b), Southern Ocean Iron Experiment (SOFeX) data are from Wanninkhof et al. (2004), SOLAS Air-Sea Gas Exchange Experiment (SAGE) data are from Ho et al. (2006), Southern Ocean Gas Exchange Experiment (SO GasEx) data from Ho et al., (2011), and Deep Ocean Gas Exchange Experiment II (DOGEE II) from Salter et al. (2011). Also shown are wind speed and gas transfer parameterizations proposed by Nightingale et al. (2000a), Ho et al. (2006), Wanninkhof et al. (2009), Wanninkhof (2014), Yang et al. (2022), Kuss et al. (2004) quadratic, Kuss et al. (2004) cubic, and Weiss et al. (2007).



Table 2. List of studies conducted in the Baltic Sea to examine carbon cycling and metabolism, along with the wind speed/gas exchange parameterization(s) that were used in each. Positive flux means flux from sea to air.

Regions	Central Baltic			Western Baltic			Baltic Sea		
	Citation	Wesslander et al. (2010)	Wessland et al. (2011)	Schneider et al. (2014)	Kuss et al. (2006)	Wesslander et al. (2010)	Thomas and Schneider (1999)	Gustafsson et al. (2014)	Laruelle et al. (2014)
Calculation period	1994-2008	April 2005	20 2009	May 2003-September 2004	1994-2008	Mean value	1989-2006	1990-2011	
Parameterization(s)	LM 86 W92	W9 WM 2 99	W09	W92 K04	LM86	W92	W09	T09	
Gas	CO ₂	CO ₂	CO ₂	CO ₂ O ₂	CO ₂ O ₂	CO ₂ CO ₂	CO ₂ CO ₂	CO ₂	CO ₂
Published Fluxes (mmol m⁻² d⁻¹)	2.6 4.5 ±14	-24 ±19 ±17	-1.6 -2.5	-8.3 ±0.5 10.8 ±3.0 -10 ±3	3.8	6.4 -2.5 ±0.25	0.98 ±0.89	0.05 (range=-4.5 and 9.1)	
Recalculated fluxes (mmol m⁻² d⁻¹)	3.7 ±12	-20 ±12	-1.7 -2.7	1.0 0				0.05 (range=-4.4 and 8.9)	

LM86, W92, WM99, K04, T09, and W09 refer to Liss and Merlivat (1986), Wanninkhof (1992), Wanninkhof and McGillis (1999), Kuss et al. (2004), Takahashi et al. (2009), and Wanninkhof et al. (2009), respectively.

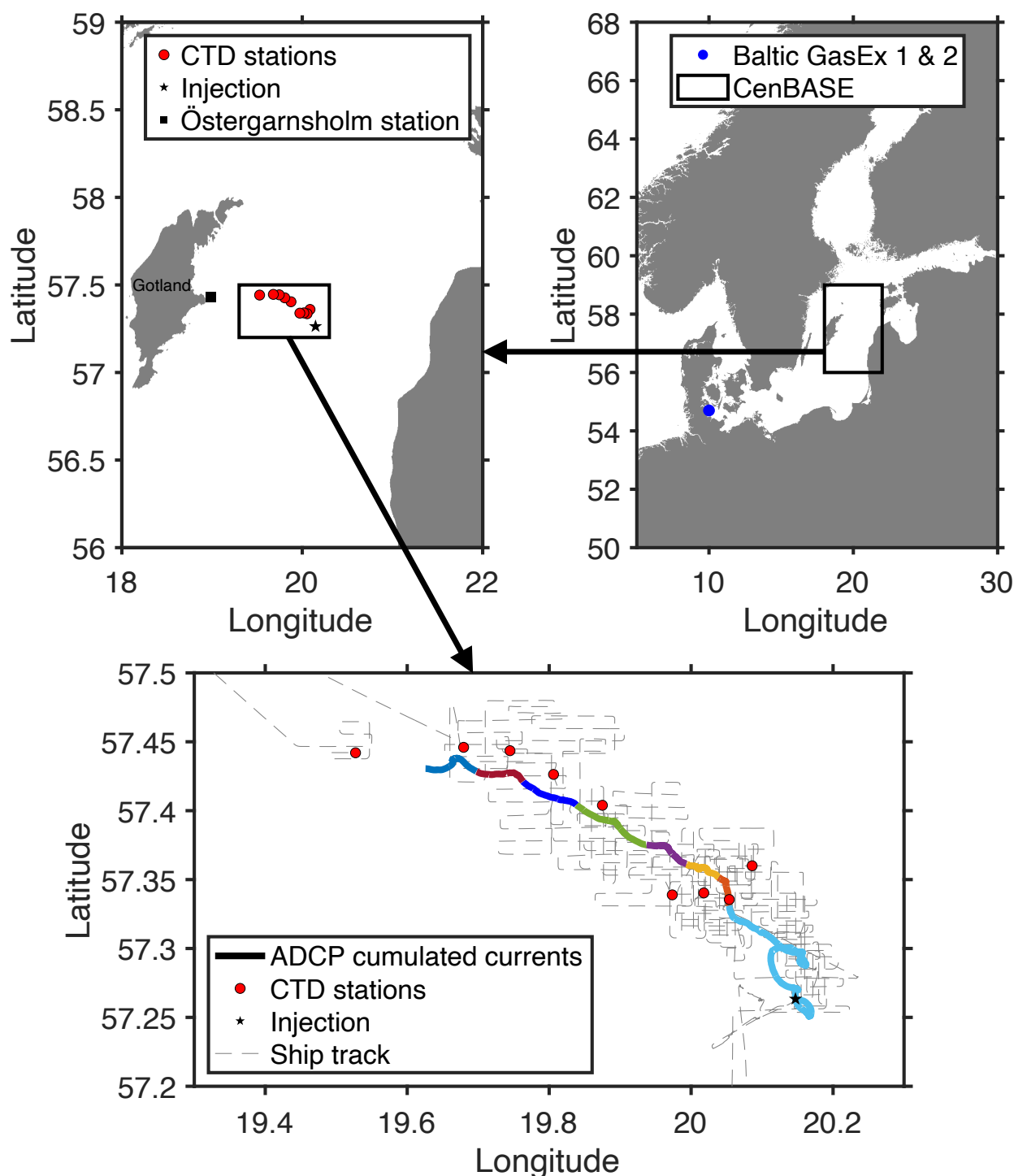


Figure 2: Location of the study area. A black star and red circles indicate the location where we injected tracers and we conducted CTD stations, respectively. In the lower panel, the thick line shows the ADCP-derived cumulated currents at approximately 4 m depth after the tracer injection, while the dashed line represents the ship track. The different colors of the ADCP line correspond to the periods between CTD stations. Map data is downloaded from GEBCO (originated from the GEBCO 2021 Grid and made with NaturalEarth by OpenDEM (2025))



transport of the injected tracers. Surfactant activity was determined to assess their influence on k . A buoy equipped with a bubble camera and temperature, salinity, and dissolved oxygen sensors at depths of 1.2 m and 2.9 m was deployed to
65 quantify the bubble distribution and dissolved oxygen concentrations.

2.2 Injection and sampling of ^3He and SF_6

On 6 July 2022 (yearday (YD) 187), ^3He and SF_6 were injected at approximately 7 m depth in a hexagonal spiral pattern with a diameter of about 1 km, centered at 57.263°N , 20.147°E (Fig. 2) over the course of 40 minutes. After the injection, an
70 underway SF_6 analysis system (Ho et al., 2002) was used to measure surface SF_6 concentrations every ~ 45 s. The surface SF_6 distribution was recorded and displayed to support ship navigation and to locate the center of the tracer patch for discrete measurements. The vessel-mounted ADCP (150 kHz Ocean Surveyor, RD Instruments) provided measurements of near-surface currents and also supported tracking the tracers (the ADCP cumulated current is shown in Fig. 2).

Approximately every 12 hours, discrete samples were taken in the water column near the center of the SF_6 patch using a
75 rosette with a conductivity, temperature, and depth (CTD) sonde and 13 5-L Niskin bottles. 250-ml syringes were used to obtain discrete SF_6 samples from the Niskin bottles. For discrete ^3He samples, about 40 ml of seawater were collected in copper tubes placed in aluminum channels. Stainless steel clamps were used to seal the tubes at both ends for later shore-based measurements.

SF_6 concentrations were measured onboard using a purge-and-trap SF_6 analysis system (Bullister and Weiss, 1988; Gerke
80 et al., 2024). This system separated SF_6 from other gases and measured its concentration by a gas chromatograph equipped with an electron capture detector (GC-ECD). Approximately 200 ml of the water sample were injected into a purge-and-trap unit. Nitrogen served as the carrier gas to purge the samples, and the gases were trapped on a 70-cm column filled with Heysep D (60/80 mesh). The trap was maintained at a temperature of approximately -70°C by suspending it over liquid nitrogen. The trapped analytes were then desorbed by heating the trap to 100°C . Separation was achieved using a 90-cm pre-
85 column filled $\frac{1}{3}$ with Porasil C and $\frac{2}{3}$ with Molsieve 5A, and a 220-cm main column, packed 90% with Carbograph 1AC and 10% with Molsieve 5A.

The ^3He samples were shipped to the laboratory at the Institute of Environmental Physics at University of Bremen for analysis. In the laboratory, after being removed from the copper tube, the samples were released into glass bulbs. From there, they were transferred into glass ampoules, which were then sealed for analysis with a helium isotope mass spectrometer
90 (MAP 215-50). $\delta^3\text{He}$ precision for ocean samples is usually better than 0.5% (Sültenfuß et al., 2009).



2.3 Physical parameters

Wind speed and direction data at a temporal resolution of 1 min were collected from the ship by a sonic anemometer (Lufft Ventus UMB). The wind speed was normalized to a reference height of 10 m, u_{10} , using the Coupled Ocean-Atmosphere Response Experiment (COARE) 3.6 algorithm (Fairall et al., 2003; Edson et al., 2013).

Although the sonic anemometer is mounted in an ideal location at the top of the foremast, the observed wind speed is still affected by distortion from the ship's superstructure. This distortion varies with the relative wind direction, with minimal impact when the wind is bow-on. To correct for the effect of the flow distortion, the ship-derived u_{10} was adjusted by referencing wind speed data from European Centre for Medium-Range Weather Forecasts Reanalysis v5 (ERA5; Hersbach et al., 2020). Before its use in the correction, the ERA5 wind speed was calibrated against a six-month record of wind speed measurements from the Östergarnsholm station (Fig. 2) (Rutgersson et al., 2020). The ship-derived u_{10} was then compared with the corrected ERA5 u_{10} at the same relative wind direction and calibrated subsequently.

A three-dimensional sonic anemometer (CSAT3B) was deployed to measure the friction velocity, u^* . Using the measured fluctuated horizontal and vertical velocity (u' and w' , respectively), u^* was determined by the following equation:

$$u_* = \sqrt{-\overline{u'w'}} \quad (1)$$

u^* was also calculated using COARE 3.6 with environmental variables, including wind and wave parameters. Since the calculated u^* was found to be generally consistent with the measured values, and the measured u^* data were not continuous, the calculated u^* was used.

Water samples for surfactant measurements were collected at the CTD stations except for YD 193, following methodologies described in Cosović and Vojvodić (1982). The sea surface microlayer was sampled using different methods depending on weather conditions: either a hydrophilic glass plate was used from a small rubber boat away from the research vessel, or a Garrett screen was deployed from the bow of the research vessel. Surfactant activity was analyzed using Polarography (797 VA Computrace Control, Metrohm, Switzerland) and referred against Triton X-100 (TX-100, Sigma-Aldrich, Germany, molecular weight 625 g mol⁻¹).

The buoy equipped with a bubble camera at a nominal depth of 80 cm was deployed on YD 185 from 09:20 to 13:55. The bubble camera is a custom-built instrument that captures high-resolution images illuminated by a strobing light sheet, and can detect bubbles with radii ranging from 0.02 to 4 mm (Al-Lashi et al., 2017). The instrument malfunctioned after this deployment, unfortunately, and preventing further deployments.

Around 2:00 UTC on YD 193, the ship left the tracer patch and headed to Gotland due to inclement weather and a medical emergency, and returned to the site around 12:00 UTC on YD 194 for one last CTD station. The corrected ERA5 wind speed data was used after YD 193.

Wave height reanalysis with a temporal resolution of 1 hour and spatial resolution of 2×2 km was obtained from the Baltic Sea wave model hindcast product (Copernicus Marine Service, 2024), and net longwave radiation flux, latent heat flux, and sensible heat flux from ERA5 were used in our study.



125

2.4 Calculation of $k(600)$

The gas transfer velocity for ^3He ($k_{^3\text{He}}$) was calculated from the change in tracer ratio over time as follows (Wanninkhof et al., 1993):

$$k_{^3\text{He}} = - \left(1 - (Sc_{\text{SF}_6} / Sc_{^3\text{He}})^{-1/2} \right)^{-1} h \frac{d}{dt} \left(\ln(^3\text{He}_{\text{exc}} / \text{SF}_6) \right) \quad (2)$$

130 Sc_{SF_6} and $Sc_{^3\text{He}}$ are the Schmidt numbers for SF_6 and ^3He , respectively, defined as the ratio of the kinematic viscosity of water to the diffusion coefficient of the gas in water (calculated following Dobashi and Ho, 2023). h denotes the tracer mixed layer depth (MLD) derived from ^3He , SF_6 , buoyancy frequency, and temperature profiles, following the methods described in Stevens et al. (2011) and Dobashi et al. (2026). $^3\text{He}_{\text{exc}}$ represents the ^3He in excess of its solubility equilibrium with the atmosphere, and is hereafter referred to simply as ^3He . The measured $k_{^3\text{He}}$ was normalized to $k(600)$, where 600 refers to Sc number of CO_2 in freshwater at 20°C , using the following relationship:

$$k(600) = k_{^3\text{He}} (600 / Sc_{^3\text{He}})^{-1/2} \quad (3)$$

$k(600)$ from equation (3) was corrected by dividing the resulting $k(600)$ by $\varepsilon = \frac{u_{10}^2}{u_{10}^2}$ to account for enhancement in $k(600)$ due to the variability in u_{10} over the observation period (Wanninkhof et al., 2004).

140 2.5 Evaluation of published parameterizations

The validity of published parameterizations in the central Baltic Sea was evaluated by comparing the observed decrease in $^3\text{He}/\text{SF}_6$ ratio with that predicted by the parameterizations. The analytical solution to Equation (2) can be written as:

$$\left(^3\text{He}/\text{SF}_6 \right)_t = \left(^3\text{He}/\text{SF}_6 \right)_{t-1} \exp \left(- \frac{k_{^3\text{He}} \Delta t}{h} \left(1 - (Sc_{\text{SF}_6} / Sc_{^3\text{He}})^{-1/2} \right) \right) \quad (4)$$

145 $(^3\text{He}/\text{SF}_6)_t$ denotes the $^3\text{He}/\text{SF}_6$ ratio at time t and $(^3\text{He}/\text{SF}_6)_{t-1}$ represents the ratio at the preceding time step. $k_{^3\text{He}}$ is calculated from measured wind speeds and the published parameterizations. Commonly used wind/ k parameterizations (Nightingale et al., 2000a; Ho et al., 2006; Wanninkhof et al., 2009; Wanninkhof, 2014), a wind and wave/ k parameterization (Reichl and Deike, 2020), high-quality eddy covariance (with a dryer to remove the water vapour)-derived parameterizations (Yang et al., 2022; Yang et al., 2024), and parameterizations specifically proposed for the Baltic Sea (Kuss et al., 2004; Weiss et al., 2007; Rutgersson and Smedman, 2010) were evaluated. The performance of these parameterizations during the observation period was assessed by comparing the predicted $^3\text{He}/\text{SF}_6$ with measured $^3\text{He}/\text{SF}_6$ using the coefficient of variation of the root mean square error (cvRMSE):

$$cvRMSE = \frac{\sqrt{\frac{1}{N} \sum_{n=1}^N (R_{mod}^n - R_{obs}^n)^2}}{R_{obs}} \quad (5)$$



R_{obs}^n and R_{mod}^n represent the observed and modeled $^3\text{He}/\text{SF}_6$ ratios, respectively. N denotes the number of stations following the initial sampling (in this study, $N=8$). This equation was also used to optimize the coefficient (A) for a quadratic
155 $(k(600)= Au_{10}^2)$ wind speed/ k parameterization, which provides a minimum cvRMSE. A was changed from 0 to 0.5 in increments of 0.001, and the A that minimized the cvRMSE was identified.

3. Results

3.1 Environmental Variables

160 The mean and standard deviation of the observed wind speed were $7.1 \pm 2.2 \text{ m s}^{-1}$ (range=1.5–12.2 m s^{-1} (Fig. 3a). Salinity was consistent throughout the study period (7.30 ± 0.01). The temperature of the air and water were $18.3 \pm 1.5^\circ\text{C}$ and $18.9 \pm 0.1^\circ\text{C}$, respectively. The surfactant activity, measured inside the tracer patch, was $0.57 \pm 0.07 \text{ mg L}^{-1}$ TX-100 equivalent (Karnatz et al. 2025). The bubble camera, which was deployed before our measurement on YD 185 for $\sim 4.5 \text{ h}$ (at $u_{10} = 6.2 \pm 2.9 \text{ m s}^{-1}$), detected no bubbles. The wave height and inverse wave age ($u_{10}/\text{wave speed}$; Ω) during the observation period
165 were $0.93 \pm 0.40 \text{ m}$ and 0.90 ± 0.28 , respectively (Fig. 3b).

3.2 Gas Transfer Velocities

The measured $k(600)$ was $10.8 \pm 2.9 \text{ cm h}^{-1}$ for the whole period (Fig. 1 and Table 3). The observed $k(600)$ was similar to offshore regions at the same wind speed. The estimated $k(600)$ derived from parameterizations for the Baltic Sea (Kuss et al.,
170 2004; Weiss et al., 2007; Rutgersson and Smedman, 2010) ranged from 11.8 to 23.0 cm h^{-1} , most of them exceeding the observed $k(600)$ (Table 1). Commonly used parameterizations (Nightingale et al., 2000a; Ho et al., 2006; Wanninkhof et al., 2009; Wanninkhof, 2014) estimated $k(600)$ ranging from 10.3 to 12.0 cm h^{-1} , which are all similar to the observed $k(600)$. The wind and wave/ k parameterization of Reichl and Deike (2020) gave an estimate of $11.9 \pm 2.7 \text{ cm h}^{-1}$, which was also close to the observed $k(600)$. The parameterization derived from open ocean high-quality eddy covariance (Yang et al., 2022;
175 Yang et al., 2024) yielded 15.9 and 16.4 cm h^{-1} , respectively, which were higher than observed $k(600)$.

Most parameterizations proposed for the Baltic Sea estimated a faster decrease in $^3\text{He}/\text{SF}_6$ and so overestimated k (Fig. 3c). This overestimation can also be observed in the cvRMSE (Table 1 and Fig. 4). The cvRMSE for parameterizations proposed specifically for the Baltic Sea ranged from 10.1% to 32.9%, which is higher than the cvRMSE of commonly used parameterizations, ranging from 6.2% to 7.3%. The cvRMSE for parameterization from eddy covariance were 18.3% and
180 19.9%, which were also higher than commonly used parameterizations. Among the published parameterizations considered in this study, the smallest cvRMSE was 5.3% from Reichl and Deike (2020) (Fig. 4).

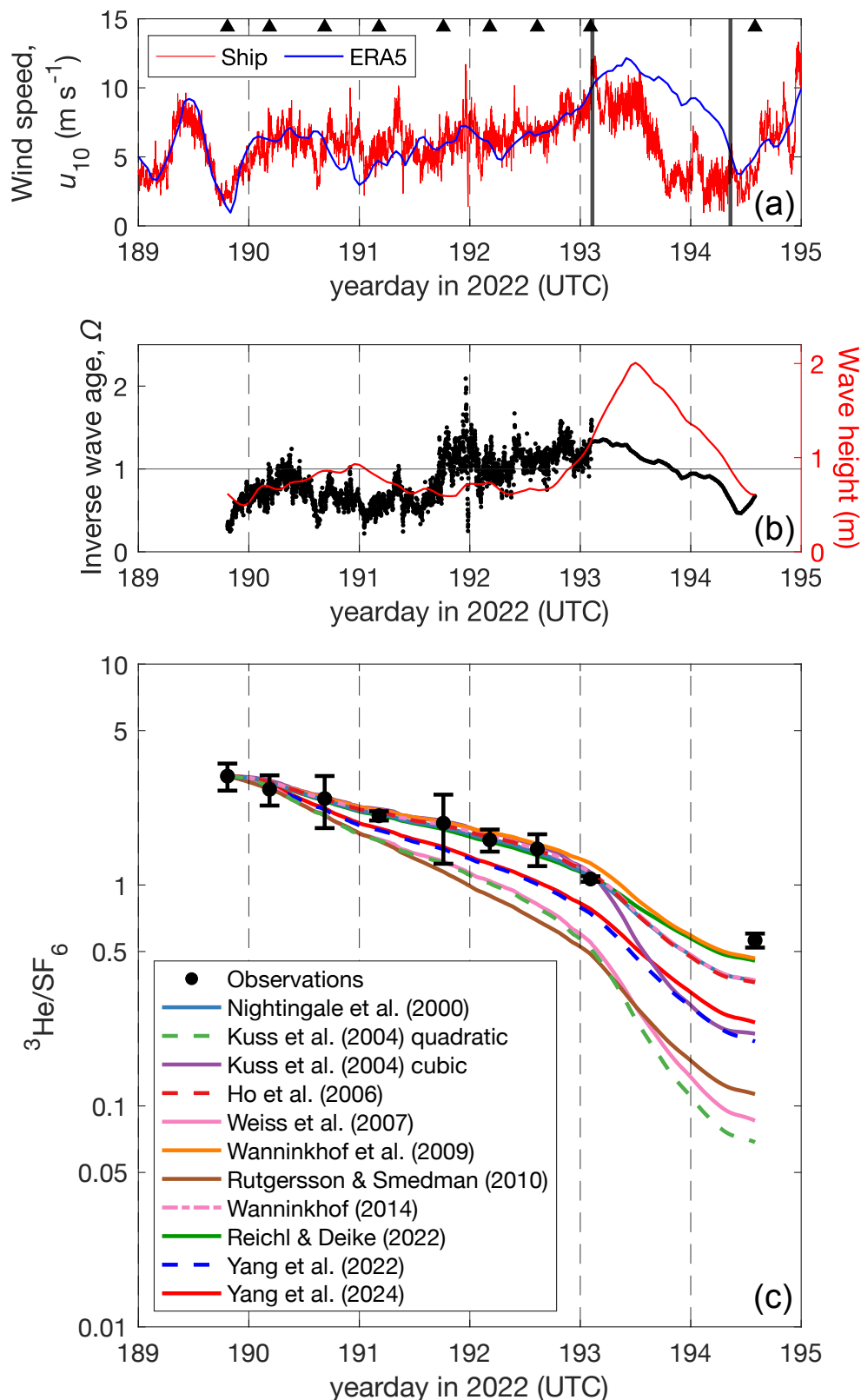


Figure 3: Time series of measurements. (a) wind speed derived from ship (red) and ERA5 (blue) at 10 m, u_{10} (units: m s^{-1}), (b) inverse wave age, Ω , defined as $u_{10}/\text{wave speed}$ (black) and wave height (units: m) (red), and (c) measured and modeled change in ${}^3\text{He}/\text{SF}_6$. The black triangle and lines in (a) denote the time of the CTD station and the duration during which we were outside the tracer patch, respectively. Error bars in (c) indicate the standard deviations. Time is written in (yearday in 2022) (UTC).



Table 3. Environmental parameters and observed $k(600)$ in this study.

u_{10} ($m s^{-1}$)	u^* from COARE 3.6 ($m s^{-1}$)	wave height (m)	inverse wave age, Ω	Observed $k(600)$ ($cm h^{-1}$)	Error in $k(600)$ ($cm h^{-1}$)	Observed $k(600)$ from Ho et al. (2006)
5.4	0.19	0.71	0.70	8.3	1.5	1.07
6.0	0.21	0.90	0.70	9.1	1.6	0.94
5.8	0.20	0.95	0.64	8.0	2.3	0.88
6.0	0.22	0.89	0.85	9.5	3.1	0.98
6.5	0.24	0.88	1.08	11.4	2.1	1.01
7.2	0.27	0.90	1.13	15.8	4.4	1.13
8.8	0.32	1.28	1.04	13.4	1.2	0.65

Error in $k(600)$ was derived from the standard error in $^3He/SF_6$ slope.

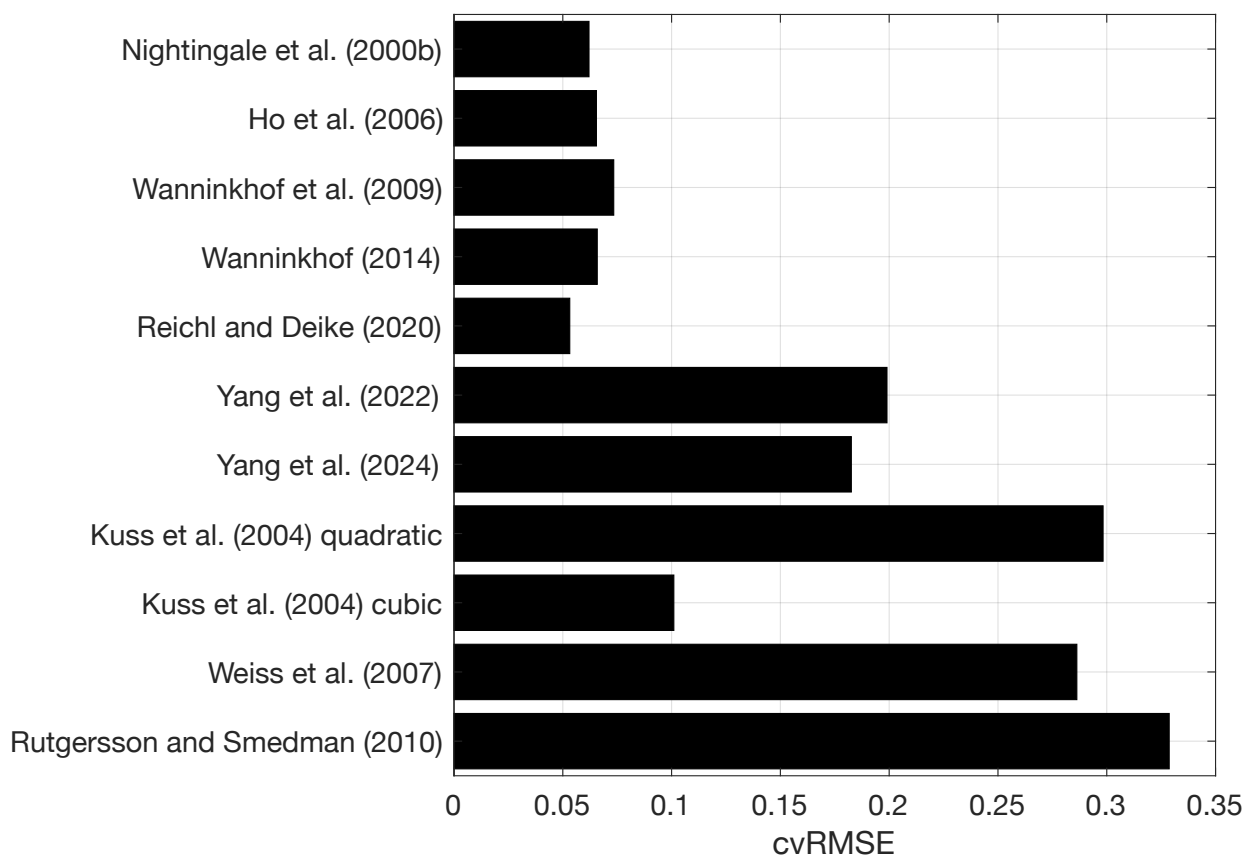


Figure 4: The cvRMSE calculated from the observed and modeled $^3\text{He}/\text{SF}_6$ by parameterizations which estimate k .



The best coefficient of quadratic parameterization was investigated based on results from this experiment, expressed as $k(600)=Au_{10}^2$, where A is a coefficient. The coefficient of minimum cvRMSE was 6.5% at $A=0.267$, which was essentially
185 identical to 0.266 proposed by Ho et al. (2006).

The ratios of observed $k(600)$ and that parameterized by Ho et al. (2006) were calculated as shown in Figure 5 and Table 3. These ratios were 0.95 ± 0.15 , close to 1, except for a value of 0.65. This comparison further indicates that Ho et al. (2006) accurately predicted the observed $k(600)$.

190 3.3 Comparison with Baltic GasEx

We referred to $k(600)$ measured during the Baltic GasEx cruises, which took place in the nearshore Baltic Sea (Fig. 2) in June and September 2018. $k(600)$ were determined using $^3\text{He}/\text{SF}_6$ (Dobashi et al., 2026). Since wave measurements were not conducted during these two cruises, Dobashi et al. (2026) used hindcast data from the same wave model employed in this study. Surfactants were also measured during Baltic GasEx (Barthelmeß and Engel, 2022).

195 During Baltic GasEx 1 and 2, $k(600)$ were $6.6 \pm 3.1 \text{ cm h}^{-1}$ and $8.0 \pm 1.2 \text{ cm h}^{-1}$, respectively, which were lower than other coastal and offshore regions at the same wind speeds, especially at the high wind speed and the young wave age (Figs. 1 and 5) (Dobashi et al., 2026). The surfactant activity was $0.30 \pm 0.03 \text{ mg-eq L}^{-1}$ and $0.35 \pm 0.05 \text{ mg-eq L}^{-1}$ during Baltic GasEx 1 and 2, respectively (Barthelmeß and Engel, 2022). These values were higher than in typical offshore areas but were lower than those observed during CenBASE.

200

4. Discussion

4.1 $k(600)$ comparison with previous measurements

The parameterizations proposed for the Baltic Sea tend to overestimate $k(600)$. Two of them were derived using EC CO_2 (Weiss et al., 2007; Rutgersson and Smedman, 2010). The fact that previous studies reported higher k in the Baltic Sea, and
205 that parameterizations derived for this region yield higher k compared to commonly used parameterizations, either indicates an enhancement of gas exchange in the Baltic Sea relative to other oceanic regions or reflects methodological differences in determining gas exchange in the Baltic Sea. Based on our results, there was no evident enhancement in k in the Baltic Sea compared with other offshore regions at the same wind speeds. Regarding methodological differences, the previous EC CO_2 data in the Baltic Sea were measured using open-path EC systems without drying the samples (Weiss et al., 2007; Rutgersson and Smedman, 2010; Gutiérrez-Loza et al., 2022), and it has been shown that water vapor will affect these
210 measurements (Landwehr et al., 2014; Blomquist et al., 2014; Nilsson et al., 2018), for which very noisy and implausible k values have been reported (e.g., Blomquist et al., 2014).

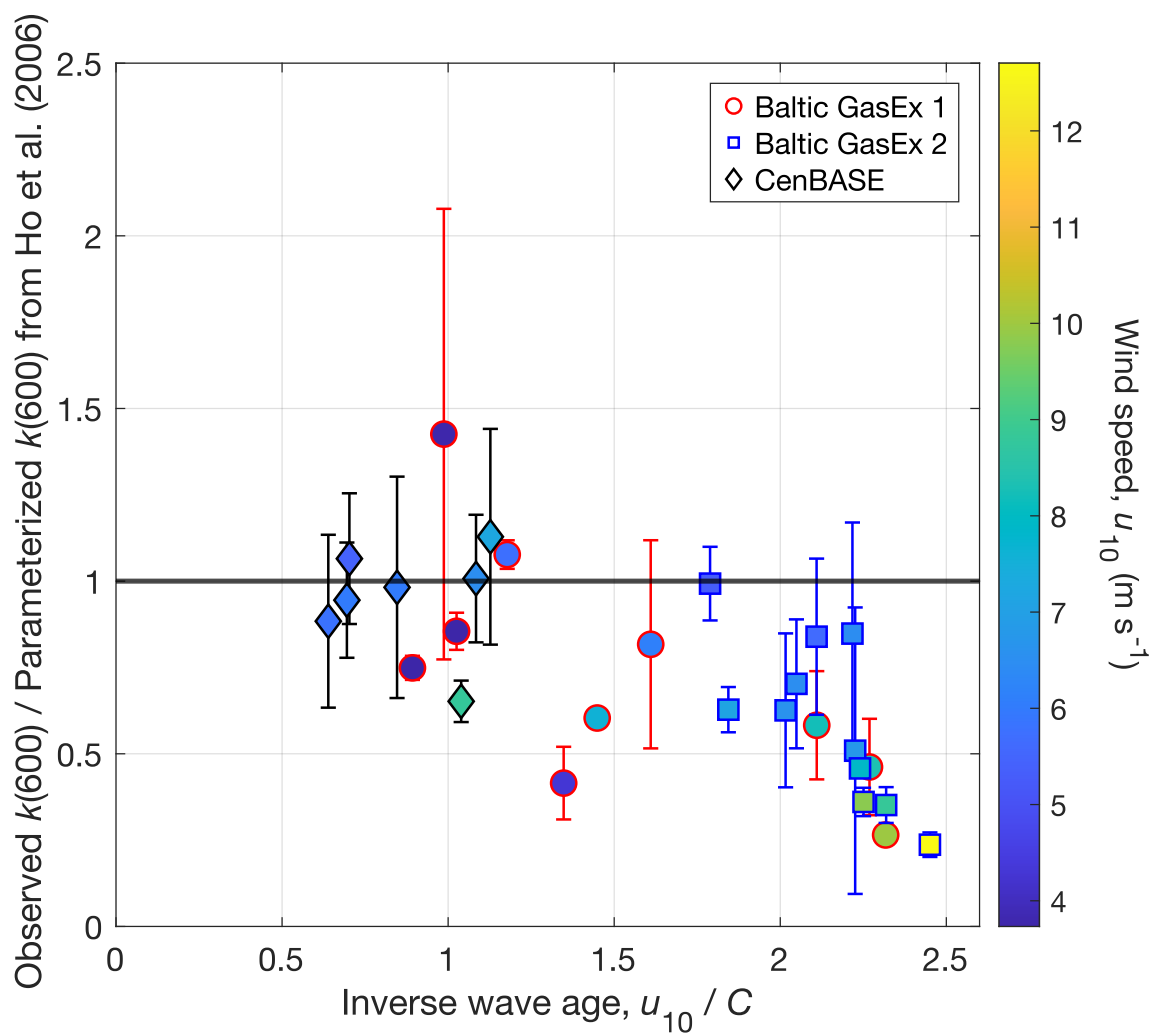


Figure 5: The ratio of observed $k(600)$ to that parameterized by Ho et al. (2006) against inverse wave age (Ω) which is defined as u_{10} /wave speed. Red circles, blue squares, and black diamonds indicate results from Baltic GasEx 1, 2, and CenBASE, respectively. Black thick line indicates the ratio equals 1.



215 The recently proposed parameterizations derived from high-quality open ocean EC CO₂ measurements (Yang et al., 2022; Yang et al., 2024) also tended to estimate a higher $k(600)$ than those observed by ³He/SF₆ in this study. The reason for this discrepancy is unclear, but it is possible that the differences observed between k derived from ³He/SF₆ and EC CO₂ in the open ocean might also exist in the Baltic Sea (Yang et al., 2022). Improvements in technology and a better understanding of errors and their corrections would contribute to a more consistent k between ³He/SF₆ tracer release experiment and EC CO₂ (Asher, 2009; Dong et al., 2021).

220 One of the parameterizations derived for the Baltic Sea was from waterside CO₂ mass balances (Kuss et al., 2004). To determine air-sea gas flux using this method, other variables, such as advection and biological activities, must be accurately calculated. Errors in these calculations propagate to air-sea gas flux, $k(600)$, and its parameterizations. Kuss et al. (2004) studied three periods, and the estimated errors in CO₂ flux calculations were 14%, 25%, and 83%, respectively. In particular, the large error during the third period is expected to have a significant impact on the calculation of $k(600)$.

225

4.2 Factors that control $k(600)$ in the Baltic Sea

Salinity was constantly 7.3 throughout the measurement period. At this salinity, the number of bubble coalescence events should be higher than in the open ocean where salinity is about 35 (Firouzi et al., 2015). The consequence is that in fresher water, bubbles will coalesce and rapidly rise to the surface, reducing both their contact time with the water and their surface area. This suggests that the salinity during our observation period may have suppressed bubble-mediated gas exchange compared with the open ocean. Also, the bubble camera deployed under a wind speed of ~6 m s⁻¹ did not detect bubbles. This suggests the number of bubbles was small and that air-sea gas exchange via bubbles was not significant. Limited fetch may have inhibited wave development, leading to a less developed wave field compared with those in the open ocean, and resulting in reduced breaking wave and bubble production.

235 We analyzed the ratio of measured to parameterized $k(600)$ by Ho et al. (2006), using data from both Baltic GasEx and CenBASE. We incrementally included data in order of increasing Ω , and calculated the mean ratio at each step. Between Ω of 0.6 and 1.8, the mean ratio was 0.9 ± 0.2 , which is close to 1. The ~10% reduction might be explained by enhanced surfactants and relatively limited fetch compared with the open ocean. However, the difference is minor given that commonly used parameterizations account for ~80% of the variance in $k(600)$ (Ho et al., 2016). This indicates that when waves have reached the fully developed phase and Ω is low, $k(600)$ can be reliably estimated by wind speed alone. In contrast, when the inverse wave age exceeded 1.8, incorporating data with higher Ω led to a decrease in the mean ratio. This indicates that when waves are in the developing phase (large Ω), for example, due to fetch limitation, $k(600)$ is smaller compared with when waves are fully developed. During CenBASE, Ω was less than 1.8 for the whole period and commonly used wind speed/ $k(600)$ parameterizations fit observed $k(600)$ well, suggesting that wind is the primary factor controlling gas exchange in this region.

245



4.3 Applicability of parameterizations

The applicability of commonly used parameterizations remains uncertain in several ecosystems and environmental conditions. The distance from the land to the observation site was approximately 70 to 340 km, implying that the fetch was limited compared with the open ocean, and so k may have been reduced. Surfactant activity during CenBASE was higher than typical open ocean concentrations (Mustaffa et al., 2020), potentially suppressing k . However, comparison with Baltic GasEx suggests that the wind/ k parameterization from Ho et al. (2006) applies well (the mean difference was about 10%) when Ω is small, even with enhanced surfactants. Therefore, our finding implies that commonly used parameterizations can be applied to other coastal and inland seas where the fetch is not strongly limited (~ 70 km) and thus Ω remains small, surfactant activity is elevated (up to $0.56 \text{ mg-eq L}^{-1}$), and wind speeds are moderate and bubbles play only a minor role.

The parameterization of Reichl and Deike (2020) yields an estimate of $k(600)$ that is about as accurate as those from commonly used parameterizations. The parameterization of Reichl and Deike (2020) was originally designed by a bubble dynamic model constrained by open ocean eddy covariance data and first proposed by Deike and Melville (2018). Reichl and Deike (2020) applied a calibration factor of 0.775 to align with Wanninkhof (2014), which explains similarities between these two parameterizations.

As summarized in Table 2, several parameterizations are applied to study biogeochemical cycles in the Baltic. We can recalculate the flux if the flux was based on $p\text{CO}_2$ measurement and k was derived from any equation with the form of $k = Au_{10}^2$, where A is an arbitrary coefficient. The recalculated k and thus fluxes are 18%, 43%, -6%, and 2% lower compared with parameterizations of Wanninkhof (1992), Kuss et al. (2004), Wanninkhof et al. (2009), and Takahashi et al. (2009), respectively. The $k(600)$ in studies applying Wanninkhof (1992) or Kuss et al. (2004) were overestimated and thus required significant corrections. In contrast, the corrections for studies that used Wanninkhof et al. (2009) and Takahashi et al. (2009) were relatively small.

Gustaffson et al. (2015) used a physical-biogeochemical model to examine the influence of parameterizations, such as k , on the calculation of air-sea CO_2 flux in the Baltic Sea. They applied wind speed/ k parameterizations of Liss and Merlivat (1986), Wanninkhof (1992), and Wanninkhof et al. (2009), and the results showed that effects on the flux were below 5%. In our study, the relationship between wind speed and k was shown to be considerably different between the nearshore and the central Baltic Sea, mainly due to fetch limitations. This study highlights the need to use different wind speed/ k parameterizations depending on wave fields, or to parameterize k not only using wind speed but also including wave field information.

275



5. Conclusion

Air-sea gas exchange in the inland sea ecosystem of the central Baltic Sea was examined using the ^3He and SF_6 dual tracer technique. Although surfactant activity was high, the observed gas transfer velocity (k) was similar to that of the open ocean at moderate wind speeds. Most parameterizations designed for the Baltic Sea tend to overpredict gas exchange, possibly due to differences in methodology. Comparison with experiments in the nearshore Baltic Sea suggests that commonly used wind speed/ k parameterizations estimate k well when wind speeds are moderate and the wave field is well-developed. Wind speed alone explains most of the variability in k in the central Baltic Sea and other inland sea ecosystems.

Data availability

Table 3 lists observed parameters. ^3He and SF_6 data are also available in Dobashi and Ho (2026).

Author contributions

RD contributed to the methodology and wrote the original manuscript. DTH led the study design and investigation, supervised the experiment, administered the project, acquired funding, and revised the manuscript. YD, CAM, and HC contributed to the methodology and revised the manuscript.

Competing interests

The authors declare that they have no conflict of interest.

Acknowledgements

We thank Benjamin Hickman for assistance in setting up the instruments, Eugene Gorman for assistance during the cruise, Toste Tanhua and Lennart Gerke for lending us their equipment, Anna Rutgersson and Erik Nilsson for providing us with the wind speed data at Östergarnsholm station, and César Sauvage and Hyodae Seo for guidance about friction velocity. Special



300 thanks to the chief scientist Henry Bittig for leading the research cruise and processing the ADCP data. The ICOS station Östergarnsholm is funded by the Swedish Research Council and Uppsala University. RD received financial support from the Crown Prince Akihito Scholarship and the Uehiro Foundation on Ethics and Education, and YD was supported by the Alexander von Humboldt Foundation. Ship time was provided by Leibniz Institute for Baltic Sea Research (IOW).

305 **Financial support**

This study was funded by the US National Science Foundation through OCE-2123997.

References

- Al-Lashi, R. S., Gunn, S. R., Webb, E. G., and Czerski, H.: A Novel High-Resolution Optical Instrument for Imaging Oceanic Bubbles, *IEEE J. Ocean. Eng.*, 43, 72–82, <https://doi.org/10.1109/JOE.2017.2660099>, 2017.
- Asher, W. E.: The effects of experimental uncertainty in parameterizing air-sea gas exchange using tracer experiment data, *Atmos. Chem. Phys.*, 9, 131–139, <https://doi.org/10.5194/acp-9-131-2009>, 2009.
- Asher, W. E. and Wanninkhof, R.: The effect of bubble-mediated gas transfer on purposeful dual-gaseous tracer experiments, *J. Geophys. Res. Oceans*, 103, 10555–10560, <https://doi.org/10.1029/98JC00245>, 1998.
- 315 Barthelmeß, T. and Engel, A.: How biogenic polymers control surfactant dynamics in the surface microlayer: Insights from a coastal Baltic Sea study, *Biogeosciences*, 19, 4965–4992, <https://doi.org/10.5194/bg-19-4965-2022>, 2022.
- Blomquist, B. W., Huebert, B. J., Fairall, C. W., Bariteau, L., Edson, J. B., Hare, J. E., and McGillis, W. R.: Advances in air-sea CO₂ flux measurement by eddy correlation, *Bound.-Layer Meteorol.*, 152, 245–276, <https://doi.org/10.1007/s10546-014-9926-2>, 2014.
- 320 Bullister, J. L. and Weiss, R. F.: Determination of CCl₃F and CCl₂F₂ in seawater and air, *Deep-Sea Res. A*, 35, 839–853, [https://doi.org/10.1016/0198-0149\(88\)90033-7](https://doi.org/10.1016/0198-0149(88)90033-7), 1988.
- Cosović, B. and Vojvodić, V.: The application of ac polarography to the determination of surface-active substances in seawater¹, *Limnol. Oceanogr.*, 27, 361–369, <https://doi.org/10.4319/lo.1982.27.2.0361>, 1982.
- Copernicus Marine Service: Baltic Sea Wave Hindcast (BALTICSEA_MULTIIYEAR_WAV_003_015), <https://marine.copernicus.eu/>, 2024.
- 325 Deike, L. and Melville, W. K.: Gas transfer by breaking waves, *Geophys. Res. Lett.*, 45, 10482–10492, <https://doi.org/10.1029/2018GL078758>, 2018.



- Dobashi, R. and Ho, D. T.: Air-sea gas exchange in a seagrass ecosystem - results from a $^3\text{He}/\text{SF}_6$ tracer release experiment, *Biogeosciences*, 20, 1075–1087, <https://doi.org/10.5194/bg-20-1075-2023>, 2023.
- 330 Dobashi, R. and Ho, D. T.: Sulfur hexafluoride and helium data from a tracer release experiment conducted in July 2022 in the central Baltic Sea during EMB295 cruise, BCO-DMO [data set], <https://doi.org/10.26008/1912/bco-dmo.988658.1>, 2026.
- Dobashi, R., Ho, D. T., Marandino, C. A., and Schlosser, P.: Air-sea gas exchange in the coastal Baltic Sea: Implications for marine carbon dioxide removal, *J. Geophys. Res. Oceans*, 131, e2025JC023324, <https://doi.org/10.1029/2025JC023324>, 2026.
- 335 Dong, Y., Yang, M., Bakker, D. C. E., Kitidis, V., and Bell, T. G.: Uncertainties in eddy covariance air–sea CO_2 flux measurements and implications for gas transfer velocity parameterisations, *Atmos. Chem. Phys.*, 21, 8089–8110, <https://doi.org/10.5194/acp-21-8089-2021>, 2021.
- Edson, J. B., Jampana, V., Weller, R. A., Bigorre, S. P., Plueddemann, A. J., Fairall, C. W., Miller, S. D., Mahrt, L., Vickers, D., and Hersbach, H.: On the exchange of momentum over the open ocean, *J. Phys. Oceanogr.*, 43, 1589–
- 340 1610, <https://doi.org/10.1175/JPO-D-12-0173.1>, 2013.
- Fairall, C. W., Bradley, E. F., Hare, J. E., Grachev, A. A., and Edson, J. B.: Bulk parameterization of air-sea fluxes: Updates and verification for the COARE algorithm, *J. Climate*, 16, 571–591, [https://doi.org/10.1175/1520-0442\(2003\)016<0571:BPOASF>2.0.CO;2](https://doi.org/10.1175/1520-0442(2003)016<0571:BPOASF>2.0.CO;2), 2003.
- Firouzi, M., Howes, T., and Nguyen, A. V.: A quantitative review of the transition salt concentration for inhibiting bubble
- 345 coalescence, *Adv. Colloid Interface Sci.*, 222, 305–318, <https://doi.org/10.1016/j.cis.2014.07.005>, 2015.
- Friedlingstein, P., O’Sullivan, M., Jones, M. W., Andrew, R. M., Hauck, J., Landschützer, P., et al.: Global Carbon Budget 2024, *Earth Syst. Sci. Data*, 17, 965–1039, <https://doi.org/10.5194/essd-17-965-2025>, 2025.
- Gerke, L., Arck, Y., and Tanhua, T.: Temporal variability of ventilation in the Eurasian Arctic Ocean, *J. Geophys. Res. Oceans*, 129, <https://doi.org/10.1029/2023JC020608>, 2024.
- 350 Gustafsson, E., Deutsch, B., Gustafsson, B. G., Humborg, C., and Mörth, C. M.: Carbon cycling in the Baltic Sea - The fate of allochthonous organic carbon and its impact on air-sea CO_2 exchange, *J. Mar. Syst.*, 129, 289–302, <https://doi.org/10.1016/j.jmarsys.2013.07.005>, 2014.
- Gustafsson, E., Omstedt, A., and Gustafsson, B. G.: The air-water CO_2 exchange of a coastal sea—a sensitivity study on factors influencing absorption and outgassing, *J. Geophys. Res. Oceans*, 120, 5342–
- 355 5357, <https://doi.org/10.1002/2015JC010832>, 2015.
- Gutiérrez-Loza, L., Nilsson, E., Wallin, M. B., Sahlée, E., and Rutgersson, A.: On physical mechanisms enhancing air-sea CO_2 exchange, *Biogeosciences*, 19, 5645–5665, <https://doi.org/10.5194/bg-19-5645-2022>, 2022.
- Hersbach, H. et al.: ERA5 hourly data on single levels from 1940 to present, Copernicus Climate Data Store [data set], <https://doi.org/10.24381/cds.adbb2d47>, 2023.
- 360 Ho, D. T. and Wanninkhof, R.: Air-sea gas exchange in the North Atlantic: $^3\text{He}/\text{SF}_6$ experiment during GasEx-98, *Tellus B*, 68, 30198, <https://doi.org/10.3402/tellusb.v68.30198>, 2016.



- Ho, D. T., Law, C. S., Smith, M. J., Schlosser, P., Harvey, M., and Hill, P.: Measurements of air-sea gas exchange at high wind speeds in the Southern Ocean: Implications for global parameterizations, *Geophys. Res. Lett.*, 33, L16601, <https://doi.org/10.1029/2006GL026817>, 2006.
- 365 Ho, D. T., Schlosser, P., and Caplow, T.: Determination of longitudinal dispersion coefficient and net advection in the tidal Hudson River with a large-scale, high resolution SF₆ tracer release experiment, *Environ. Sci. Technol.*, 36, 3234–3241, <https://doi.org/10.1021/es015814+>, 2002.
- Ho, D. T., Wanninkhof, R., Schlosser, P., Ullman, D. S., Hebert, D., and Sullivan, K. F.: Toward a universal relationship between wind speed and gas exchange: Measurements with ³He/SF₆ during the Southern Ocean Gas Exchange Experiment, *J. Geophys. Res. Oceans*, 116, C00F04, <https://doi.org/10.1029/2010JC006854>, 2011.
- 370 Karnatz, J., Barthelmeß, T., Sabbaghzadeh, B., and Engel, A.: Biochemical characteristics of the sea surface microlayer in the central Baltic Sea and potential signatures of cyanobacterial blooms, *EGUsphere* [preprint], <https://doi.org/10.5194/egusphere-2025-5385>, 2025.
- Kuliński, K., Rehder, G., Asmala, E., Bartosova, A., Carstensen, J., Gustafsson, B., Hall, P. O. J., Humborg, C., Jilbert, T., 375 Jürgens, K., Meier, H. E. M., Müller-Karulis, B., Naumann, M., Olesen, J. E., Savchuk, O., Schramm, A., Slomp, C. P., Sofiev, M., Sobek, A., Szymczycha, B., and Undeman, E.: Biogeochemical functioning of the Baltic Sea, *Earth Syst. Dyn.*, 13, 633–685, <https://doi.org/10.5194/esd-13-633-2022>, 2022.
- Kuss, J., Nagel, K., and Schneider, B.: Evidence from the Baltic Sea for an enhanced CO₂ air-sea transfer velocity, *Tellus B*, 56, 175, <https://doi.org/10.3402/tellusb.v56i2.16407>, 2004.
- 380 Kuss, J., Roeder, W., Wlost, K. P., and DeGrandpre, M. D.: Time-series of surface water CO₂ and oxygen measurements on a platform in the central Arkona Sea (Baltic Sea), *Mar. Chem.*, 101, 220–232, <https://doi.org/10.1016/j.marchem.2006.03.004>, 2006.
- Landwehr, S., Miller, S. D., Smith, M. J., Saltzman, E. S., and Ward, B.: Analysis of the PKT correction for direct CO₂ flux measurements over the ocean, *Atmos. Chem. Phys.*, 14, 3361–3372, <https://doi.org/10.5194/acp-14-3361-2014>, 2014.
- 385 Liss, P. S. and Merlivat, L.: Air-sea gas exchange rates: Introduction and synthesis, in: *The role of air-sea exchange in geochemical cycling*, Springer, 113–127, https://doi.org/10.1007/978-94-009-4738-2_5, 1986.
- Mustaffa, N. I. H., Ribas-Ribas, M., Banko-Kubis, H. M., and Wurl, O.: Global reduction of in situ CO₂ transfer velocity by natural surfactants in the sea-surface microlayer, *Proc. R. Soc. A*, 476, 20190763, <https://doi.org/10.1098/rspa.2019.0763>, 2020.
- 390 McGillis, W. R., Edson, J. B., Hare, J. E., and Fairall, C. W.: Direct covariance air-sea CO₂ fluxes, *J. Geophys. Res.*, 106, 16729–16745, <https://doi.org/10.1029/2000JC000506>, 2001.
- Nightingale, P. D., Liss, P. S., and Schlosser, P.: Measurements of air-sea gas transfer during an open ocean algal bloom, *Geophys. Res. Lett.*, 27, 2117–2120, <https://doi.org/10.1029/2000GL011541>, 2000b.



- Nightingale, P. D., Malin, G., Law, C. S., Watson, A. J., Liss, P. S., Liddicoat, M. I., Boutin, J., and Upstill-Goddard, R. C.:
395 In situ evaluation of air-sea gas exchange parameterizations using tracers, *Glob. Biogeochem. Cycles*, 14, 373–
387, <https://doi.org/10.1029/1999GB900091>, 2000a.
- Nilsson, E., Bergström, H., Rutgersson, A., Podgrajsek, E., Wallin, M. B., Bergström, G., Dellwik, E., Landwehr, S., and
Ward, B.: Evaluating humidity and sea salt disturbances on CO₂ flux measurements, *J. Atmos. Ocean. Technol.*, 35, 859–
875, <https://doi.org/10.1175/JTECH-D-17-0072.1>, 2018.
- 400 OpenDEM: Bathymetry (derived from GEBCO 2021 grid), https://opendem.info/download_bathymetry.html, 2025.
- Reichl, B. G. and Deike, L.: Contribution of sea-state dependent bubbles to air-sea carbon dioxide fluxes, *Geophys. Res.
Lett.*, 47, e2020GL087267, <https://doi.org/10.1029/2020GL087267>, 2020.
- Rutgersson, A., Pettersson, H., Nilsson, E., Bergström, H., Wallin, M. B., Nilsson, E. D., Sahlée, E., Wu, L., and
Mårtensson, E. M.: Using land-based stations for air-sea interaction studies, *Tellus A*, 72, 1–
405 23, <https://doi.org/10.1080/16000870.2019.1697601>, 2020.
- Rutgersson, A. and Smedman, A.: Enhanced air-sea CO₂ transfer due to water-side convection, *J. Mar. Syst.*, 80, 125–
134, <https://doi.org/10.1016/j.jmarsys.2009.11.004>, 2010.
- Salter, M. E., Upstill-Goddard, R. C., Nightingale, P. D., Archer, S. D., Blomquist, B. W., Ho, D. T., Huebert, B. J.,
Schlosser, P., and Yang, M.: Impact of an artificial surfactant release on air-sea gas fluxes during the Deep Ocean Gas
410 Exchange Experiment II, *J. Geophys. Res. Oceans*, 116, C11023, <https://doi.org/10.1029/2011JC007023>, 2011.
- Stevens, C., Ward, B., Law, C., and Walkington, M.: Surface layer mixing during the SAGE ocean fertilization experiment,
Deep-Sea Res. II, 58, 776–785, <https://doi.org/10.1016/j.dsr2.2010.10.017>, 2011.
- Sültenfuß, J., Roether, W., and Rhein, M.: The Bremen mass spectrometric facility for the measurement of helium isotopes,
neon, and tritium in water, *Isotopes Environ. Health Stud.*, 45, 83–95, <https://doi.org/10.1080/10256010902871929>, 2009.
- 415 Takahashi, T., Sutherland, S. C., Wanninkhof, R., Sweeney, C., Feely, R. A., Chipman, D. W., Hales, B., Friederich, G.,
Chavez, F., Sabine, C., Watson, A., Bakker, D. C. E., Schuster, U., Metzl, N., Yoshikawa-Inoue, H., Ishii, M., Midorikawa,
T., Nojiri, Y., Körtzinger, A., Steinhoff, T., Hoppema, M., Olafsson, J., Arnarson, T. S., Tilbrook, B., Johannessen, T.,
Olsen, A., Bellerby, R., Wong, C. S., Delille, B., Bates, N. R., and de Baar, H. J. W.: Climatological mean and decadal
change in surface ocean pCO₂, and net sea-air CO₂ flux over the global oceans, *Deep-Sea Res. II*, 56, 554–
420 577, <https://doi.org/10.1016/j.dsr2.2008.12.009>, 2009.
- Thomas, H. and Schneider, B.: The seasonal cycle of carbon dioxide in Baltic Sea surface waters, *J. Mar. Syst.*, 22, 53–
67, [https://doi.org/10.1016/S0924-7963\(99\)00030-5](https://doi.org/10.1016/S0924-7963(99)00030-5), 1999.
- Wanninkhof, R.: Relationship between wind speed and gas exchange over the ocean, *J. Geophys. Res.*, 97, 7373–
7382, <https://doi.org/10.1029/92JC00188>, 1992.
- 425 Wanninkhof, R.: Relationship between wind speed and gas exchange over the ocean revisited, *Limnol. Oceanogr. Methods*,
12, 351–362, <https://doi.org/10.4319/lom.2014.12.351>, 2014.



Wanninkhof, R. and McGillis, W. R.: A cubic relationship between wind speed and gas exchange, *Geophys. Res. Lett.*, 26, 1889–1892, <https://doi.org/10.1029/1999GL900363>, 1999.

430 Weiss, A., Kuss, J., Peters, G., and Schneider, B.: Evaluating transfer velocity–wind speed relationship using eddy covariance CO₂ fluxes, *J. Mar. Syst.*, 66, 130–139, <https://doi.org/10.1016/j.jmarsys.2006.04.011>, 2007.

Wesslander, K., Hall, P. O. J., Hjalmarsson, S., Lefèvre, D., Omstedt, A., Rutgersson, A., Sahlée, E., and Tengberg, A.: Observed carbon dioxide and oxygen dynamics in a Baltic Sea coastal region, *J. Mar. Syst.*, 86, 1–9, <https://doi.org/10.1016/j.jmarsys.2011.01.001>, 2011.

435 Yang, M., Bell, T. G., Bidlot, J. R., Blomquist, B. W., Butterworth, B. J., Dong, Y., Fairall, C. W., Landwehr, S., Marandino, C. A., Miller, S. D., Saltzman, E. S., and Zavarisky, A.: Global synthesis of air-sea CO₂ transfer velocity estimates from ship-based eddy covariance measurements, *Front. Mar. Sci.*, 9, 826421, <https://doi.org/10.3389/fmars.2022.826421>, 2022.

Yang, M., Moffat, D., Dong, Y., and Bidlot, J. R.: Deciphering variability in air-sea gas transfer due to sea state and wind history, *PNAS Nexus*, 3, pgae389, <https://doi.org/10.1093/pnasnexus/pgae389>, 2024.

440